Journal of Catalysis 331 (2015) 25–38

Contents lists available at ScienceDirect

Journal of Catalysis

journal homepage: www.elsevier.com/locate/jcat

Effects of Si/Al ratio on Cu/SSZ-13 NH_3-SCR catalysts: Implications for the active Cu species and the roles of Brønsted acidity

Feng Gao *, Nancy M. Washton, Yilin Wang, Márton Kollár, János Szanyi, Charles H.F. Peden *

Institute for Integrated Catalysis, Pacific Northwest National Laboratory, P.O. Box 999, Richland, WA 99352, United States

ARTICLE INFO

Article history:
Received 23 April 2015
Revised 27 July 2015
Accepted 11 August 2015
Available online 3 September 2015

Keywords:
Selective catalytic reduction
Cu/SSZ-13
Si/Al ratio
NMR
Temperature-programmed desorption
Reaction kinetics

ABSTRACT

Cu/SSZ-13 catalysts with three Si/Al ratios of 6, 12 and 35 were synthesized with Cu incorporation via solution ion exchange. The implications of varying Si/Al ratios on the nature of the multiple Cu species that can be present in the SSZ-13 zeolite are a major focus of this work, as highlighted by the results of a variety of catalyst characterization and reaction kinetics measurements. Specifically, catalysts were characterized with surface area/pore volume measurements, temperature programmed reduction by H_2 (H_2-TPR), NH_3 temperature programmed desorption (NH_3-TPD), and DRIFTS and solid-state nuclear magnetic resonance (NMR) spectroscopies. Catalytic properties were examined using NO oxidation, ammonia oxidation, and standard ammonia selective catalytic reduction (NH_3-SCR) reactions on selected catalysts under differential conditions. Besides indicating the possibility of multiple active Cu species for these reactions, the measurements are also used to untangle some of the complexities caused by the interplay between redox of Cu ion centers and Brønsted acidity. All three reactions appear to follow a redox reaction mechanism, yet the roles of Brønsted acidity are quite different. For NO oxidation, increasing Si/Al ratio lowers Cu redox barriers, thus enhancing reaction rates. Brønsted acidity appears to play essentially no role for this reaction. For standard NH_3-SCR, residual Brønsted acidity plays a significant beneficial role at both low- and high-temperature regimes. For NH_3 oxidation, no clear trend is observed suggesting both Cu ion center redox and Brønsted acidity play important and perhaps competing roles.

1. Introduction

The mechanism for ammonia selective catalytic reduction (NH_3-SCR) over Cu ion exchanged zeolite catalysts is still widely debated. Some key points of disagreement are as follows. (1) Whether the catalytically relevant Cu species are monomeric or dimeric (even, perhaps, very small Cu ion clusters) [1–3]. (2) Which NO_x and NH_x species are most relevant in the formation of key reaction intermediates? Specifically, whether NO oxidation to NO_2 is an indispensable step in standard SCR [2,4–6], and which NH_x species, NH_4^+, molecular NH_3, or even $NH_{2(a)}$, is the most relevant reductant? (3) Which reaction mechanism best describes NH_3-SCR? In particular, Langmuir–Hinshelwood, Eley–Rideal, and Mars van Krevelen (redox) mechanisms have been previously proposed for NH_3-SCR [7]. Note specifically that most prior mechanistic understanding for NH_3-SCR has been derived from the exhaustively studied VO_x/TiO_2 system. However, the applicability of such knowledge to the zeolite system is questionable since the latter has different catalytically active centers, much higher NH_3 storage capabilities and unique structural characteristics (confinement at a nanometer scale that also gives rise to electrostatic field effects). Most recently, the involvement of redox of metal ions as part of the reaction mechanism, seems to gain common agreement for zeolite-based catalysts [8–10]. (4) Whether Cu/CHA are dual functional in SCR; that is, whether both Cu ion sites and Brønsted acid sites collectively provide the catalytic functionality.

There have been numerous recent studies on the nature of Cu catalytic centers in Cu/SSZ-13 [9–20]. Cu has been suggested to stay predominately as isolated Cu^{2+} ions in SSZ-13; under dehydrated conditions they prefer windows of 6MR as noted above. However, depending on the Al content/distribution and Cu loading, even when only isolated Cu^{2+} ions are considered, there is still a high degree of complexity regarding their locations [10,13–15]. For example, at relatively low Si/Al ratios and low Cu loadings, one expects that (again, in dehydrated form) the majority of isolated Cu^{2+} ions reside near the windows of 6MR and bind with 2 Al T-sites [11,16]. In contrast, at very high Si/Al ratios where the possibility for finding 2 Al sites in one 6MR is highly unlikely, it is possible that isolated Cu^{2+} ions will interact with 2 Al sites that are farther apart (e.g.,. 2 Al sites in one 8MR). Alternatively, Cu ions

* Corresponding authors.
E-mail addresses: feng.gao@pnnl.gov (F. Gao), chuck.peden@pnnl.gov (C.H.F. Peden) .

http://dx.doi.org/10.1016/j.jcat.2015.08.004

at high Si/Al ratios may charge-balance only one Al site. In this latter case, $[Cu^{II}(OH)]^+$ or Cu^+ species are required in order to appropriately balance the negative framework charge [21]. Recently, Andersen et al. [22] studied the location of Cu^{2+} in CHA zeolite by X-ray diffraction using the Rietveld/maximum entropy method. These authors confirmed the presence of $[Cu^{II}(OH)]^+$ located in windows of 8MRs for high Cu-loaded Cu/SSZ-13, a notion fully consistent with theoretical studies [23].

Very recently, we conducted a detailed kinetic study of NH_3-SCR and two relevant reactions – i.e., NO and NH_3 oxidation – on a series of Cu/SSZ-13 catalysts with Si/Al = 6 and various Cu/Al ratios [10]. In terms of the nature of catalytically active Cu species, our results suggested the following key findings. (1) Below a reaction temperature of ~300 °C, strong solvation effects from H_2O and NH_3 render high mobility for isolated Cu^{2+} ions such that transient Cu-ion dimers form (in equilibrium with monomers) at low to intermediate Cu loadings. These transient dimeric species are catalytically relevant for standard NH_3-SCR and NH_3 oxidation reactions. (2) For standard NH_3-SCR, Cu-ion monomers are also catalytically active and even become the dominant catalytic centers at intermediate Cu loadings below ~300 °C. However, low-temperature active monomers are not located at windows of 6-membered rings (6MR). (3) Cu-ion monomers migrate to windows of 6MR at elevated reaction temperatures (>350 °C) and become the high-temperature catalytically relevant species. Because of the high redox barriers for Cu ion monomers in these locations, NH_3-SCR is characterized by high apparent reaction activation energies (~140 kJ/mol), much higher than typical apparent activation energies obtained on Cu/SSZ-13 zeolites at lower temperatures [9,15]. (4) At high Cu loadings (more than one Cu^{2+} ion per unit cell), permanent Cu-ion dimers form under SCR reaction conditions. While these moieties are active in NO oxidation to NO_2 and are believed to be (even highly) active for NH_3-SCR, they do not appear to improve catalyst performance. This can be rationalized by internal mass transfer limitations induced by these species since they both block pore openings and occupy space within CHA cages.

Overall, the interplay between Cu ion loading, Cu ion mobility and reaction temperature makes the entire NH_3-SCR reaction network quite complicated. Indeed, SCR catalysis is further influenced by CHA zeolite Si/Al ratios, and the effects are at least twofold: Si/Al ratios affect Cu ion locations as briefly discussed above, as well as significantly altering Brønsted acidity and, therefore, NH_3 storage of the catalysts. With regard to the roles of Brønsted acidity in SCR, the literature has been rather controversial. For V_2O_5-based SCR catalysts, reactive NH_3 in the form of NH_4^+ has been frequently proposed [7,24–27]. In explaining the beneficial effects of low Si/Al ratio to SCR on zeolite-based SCR catalysts, Yang and coworkers adapted the same argument and proposed that this is because more NH_4^+ species are formed at lower Si/Al ratios (i.e., more Brønsted acid sites) [28,29]. However, titration experiments in a few recent studies on Cu/CHA catalysts demonstrate that NH_4^+ species are far less reactive toward NO_x than molecular NH_3 adsorbed on Cu sites [30–32]. Interestingly, in V_2O_5-based catalysts, NH_4^+ binds to the catalysts more weakly than NH_3 adsorbed on Lewis acid sites [7], while it is the opposite for zeolite-based catalysts. Therefore, if one makes the reasonable argument that more weakly bound NH_x species are more reactive, consistency still maintains for the two classes of catalysts. In any case, for zeolite-based SCR catalysts, Brønsted acidity may be expected to influence the reaction by affecting Cu ion location and NH_3 storage (the latter plays a more significant role under transient rather than steady-state reaction conditions), rather than the formation of reactive NH_4^+. Indeed, in recent studies by Bates et al. [9,33] on a series of Cu/SCR rates on the number of residual Brønsted acid sites measured from NH_3 titration. In our recent study, TOFs were also found to be largely insensitive to Cu/Al ratios under certain reaction conditions [10]. Note, however, that this zero-order dependence on Brønsted acidity may not be general: using samples with the same Si/Al ratio and a narrow range of low Cu/Al ratios (<0.2), the numbers of residual Brønsted acid sites in different samples are not expected to vary dramatically to allow reliable correlations between SCR rate and Brønsted acid density.

Importantly, correlation between SCR rates and residual Brønsted acid density requires the latter to be quantified *in situ* (i.e., under SCR reaction conditions). This is experimentally challenging. Recently, Gounder and coworkers developed protocols for *ex situ* quantification of Brønsted acid sites using NH_3-TPD [33,34]. These authors showed that, for Cu/SSZ-13 samples with high Al content and low Cu/Al ratios, Brønsted acid sites are exchanged by Cu^{2+} ions stoichiometrically (i.e., $2H^+$ per Cu^{2+}). However, this trend does not extend to high Cu loadings and is suggested to be due to the formation of Cu_xO_y clusters that do not play a charge-balancing role [34]. Recent studies by others also revealed the presence of substantial residual Brønsted acid sites in Cu/SSZ-13 at high Cu loadings. For example, one study by Giordanino et al. [35] determined that Brønsted sites are still present even if the Cu/Al ratio is not far from the stoichiometric exchange level. They suggested that some of the Brønsted sites are exchanged by monovalent copper complexes $[CuOH]^+$. In another study, Lezcano-Gonzalez et al. [31] showed that the intensity of ν_{OH} vibrations (bands at 3605 and 3585 cm^{-1} assigned to Brønsted acid sites) in their Cu/SSZ-13 sample at a 100% ion exchange level (i.e., Cu/Al = 0.5), was still comparable to their parent H/SSZ-13.

Clearly, from the recent publications described above, there is still much to learn about the nature of Cu ion species and the roles of Brønsted acidity in Cu/SSZ-13 SCR catalysts. For example, a catalytic property comparison between Cu^{2+} and $[Cu(OH)]^+$ active sites has not yet been established and SCR performance between catalysts with vastly different Brønsted acid site densities has not yet been studied. In the present study, we aim to obtain a more general picture on the roles of Cu ion location and Brønsted acidity in NH_3-SCR by using a relatively large number of samples with various Si/Al and Cu/Al ratios.

2. Experimental

2.1. Catalyst synthesis

Based on the above considerations, three SSZ-13 substrates with different Si/Al ratios were synthesized and used in the present study. The synthesis for SSZ-13 with Si/Al = 6 via a static hydrothermal method has been described in detail elsewhere [11,12] and will not be repeated here. For the two higher Si/Al ratio samples, synthesis was conducted hydrothermally under stirring using a method modified from a protocol developed recently by Deka et al. [16]. Composition of the gel is as follows: 10SDA:10-NaOH:$x$$Al_2O_3$:100$SiO_2$:2200$H_2O$, where x varies to allow preparation of samples with different Si/Al ratios. The gel is prepared first by dissolving NaOH (99.95%, Aldrich) in water and adding the SDA (TMAda-OH, Sachem ZeoGen 2825). Following which, Al $(OH)_3$ (contains ~54% Al_2O_3, Aldrich) and fumed silica (0.007 μm average particle size, Aldrich) were added sequentially under vigorous stirring until the gel was homogenized. The gel was then sealed into a 125 ml Teflon-lined stainless steel autoclave with a stir bar in. Thereafter, the autoclave was placed in a salt bath on

hydrothermal synthesis was very critical for the formation of uniform and highly crystallized SSZ-13 in this method. After synthesis, Na/SSZ-13 was separated from the mother liquid via centrifugation and washed with deionized water 3 times. Finally, the zeolite powders were dried at 120 °C under flowing N_2, and calcined in air for 8 h to remove the SDA (calcination temperatures detailed below). Si and Al contents of the product powders were measured with Inductively Coupled Plasma Atomic Emission Spectroscopy (ICP-AES) at Galbraith Laboratories (Knoxville, TN, USA). Prior to these composition measurements, the samples were dehydrated at 150 °C for 2 h in vacuum to remove adsorbed moisture. The Si and Al weight contents, as well as the Si/Al molar ratios thus derived, are listed in Table 1. For the Si/Al = 6 and 12 samples, a calcination temperature of 550 °C is sufficient to completely burn off the SDA. However, for the Si/Al = 35 sample, a calcination temperature of 650 °C is required. One likely explanation is that sodium promotes SDA combustion, and this sample contains much less Na than the lower Si/Al samples. XRD patterns and SEM images of the calcined samples are shown in Supplementary Information (SI-1 and SI-2, respectively). Solid-state nuclear magnetic resonance (NMR) analysis of the calcined samples was conducted on a Varian VNMRS system. Experimental details can be found elsewhere [36]. Cu/SSZ-13 samples were prepared using a standard two-step solution ion exchange protocol reported previously, first with NH_4NO_3 followed by $CuSO_4$ solutions at 80 °C [15].

2.2. Catalyst characterization

Cu contents of the Cu/SSZ-13 samples were also determined with ICP-AES. Table 2 presents Cu weight percentages, and the corresponding Cu/Al molar ratios and ion exchange levels for all Cu/SSZ-13 samples used in the present study. In the following text, in cases where only one measure of Cu loading is provided, the others can be readily found in this table. BET surface areas and micropore volumes of the samples were measured with a Quantachrome Autosorb-6 analyzer. Prior to analysis, the samples were dehydrated under vacuum overnight at 250 °C. For all of the samples studied here, BET surface areas are 500–550 m^2/g and micropore volumes are ~0.25 cm^3/g. Temperature-programmed reduction (TPR) was performed on a Micromeritics AutoChem II analyzer. TPR was carried out on both hydrated samples (samples stored in air and saturated with moisture) and fully dehydrated samples (samples calcined at 550 °C in 5% O_2/He flow for 30 min and cooled to ambient temperature in the same flow). Typically ~50 mg of sample was used for each measurement. TPR was carried out in 5% H_2/Ar at a flow rate of 30 ml/min. Temperature was ramped linearly from ambient to 650 °C at 10 °C/min and H_2 consumption was monitored with a TCD detector. A water condenser was applied in front of the TCD detector to trap H_2O within the outlet stream. Powder X-ray diffraction (XRD) measurements were performed on a Philips PW3040/00 X'Pert powder X-ray diffractometer with Cu K_α radiation (λ = 1.5406 Å). Data were collected with 2θ ranging from 5° to 50° using a step size of 0.02°. Scanning Electron Microscopy (SEM) was conducted on a FEI Helios 600 FIB-SEM instrument. Samples were mounted on a carbon tape and 5 nm of carbon was deposited onto the samples for conductivity. Imaging was done at 5 keV.

Table 1
Si and Al contents and corresponding Si/Al ratios for the 3 SSZ-13 samples.

Sample	Si content (wt.%)	Al content (wt.%)	Si/Al ratio
1	30.4	5.03	6
2	40.3	3.23	12
3	43.4	1.20	35

Table 2
Cu contents, and corresponding Cu/Al ratios and ion exchange levels for all of the Cu/SSZ-13 samples (in dehydrated form) used in this study.

Sample	Cu content (wt.%)	Cu/Al ratio	Ion exchange level (%)[a]
Cu/SSZ-13 (Si/Al = 6)	0.065	0.006	1.1
	0.095	0.008	1.6
	0.188	0.016	3.2
	0.378	0.032	6.4
	0.516	0.044	8.7
	1.31	0.11	22
	2.59	0.22	44
	3.43	0.29	58
	4.67	0.40	79
	5.15	0.44	87
Cu/SSZ-13 (Si/Al = 12)	0.48	0.06	13
	1.00	0.13	26
	1.74	0.23	46
Cu/SSZ-13 (Si/Al = 35)	0.28	0.10	20
	0.64	0.23	45

NH_3 temperature programmed desorption (NH_3-TPD) was used to quantify Brønsted acid sites in the H/SSZ-13 samples, as well as to describe NH_3 adsorption on Lewis and Brønsted acid sites in the Cu/SSZ-13 catalysts. NH_3-TPD was carried out using our SCR reaction system, with NH_3 detection via gas-phase FTIR. 60 mg catalyst (60–80 mesh) was used for each measurement and the following experimental steps were followed: (1) Heat the sample to 550 °C in O_2/N_2 (300 sccm, 14% O_2) and keep at 550 °C for 30 min; (2) stop O_2 flow, maintain N_2 flow, and cool sample to NH_3 adsorption temperatures (defined below); (3) adsorb NH_3 (~500 ppm in N_2) until outlet NH_3 concentration stays constant for 1 h; (4) turn off the NH_3 flow and purge with N_2 for 1 h at the adsorption temperature; and (5) ramp from the adsorption temperature to 600 °C at 10 °C/min, and maintain at 600 °C until NH_3 desorption is complete. For the quantification of Brønsted acid sites in the H/SSZ-13 samples, the NH_3 adsorption and purging temperature were set at 200 °C to avoid weakly-bound NH_3. For the Lewis/Brønsted site titrations in Cu/SSZ-13 catalysts, the NH_3 adsorption and purging temperature were set at 100 °C. Stretching vibrations of Brønsted acid sites (ν_{OH}) were probed with DRIFT spectroscopy as described previously [30]. After the sample was loaded into the ceramic sample holder cup of a high temperature/high pressure cell, it was dehydrated at 550 °C for 1 h in flowing helium (10 ml/min). After that, the sample was cooled to 227 °C under flowing helium prior to spectrum acquisition. Spectra were ratioed to a background spectrum collected of KBr at the same temperature.

2.3. SCR and NO/NH_3 oxidation reaction tests

NH_3-SCR and NO/NH_3 oxidation kinetics measurements were carried out in a plug-flow reaction system. Experimental details and mathematic equations used for data analysis are given elsewhere [10,15]. Specifically, all kinetic data for detailed analyses were judged kinetically benign using the Koros–Nowak criterion [9,10], and the NH_3-SCR data were further corrected assuming first-order kinetics.

3. Results

3.1. Solid-state nuclear magnetic resonance (NMR) results

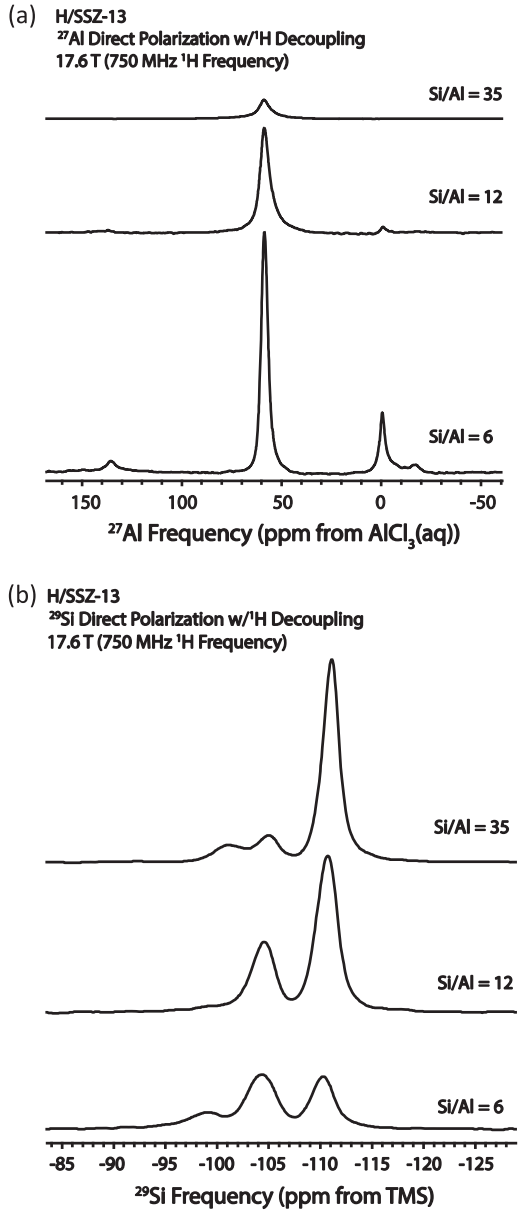

Fig. 1. Solid state (a) ^{27}Al and (b) ^{31}Si NMR spectra for the H/SSZ-13 samples with Si/Al ratio = 6, 12 and 35. Samples were prepared by ion-exchanging Na/SSZ-13 samples to NH_4/SSZ-13 followed by a calcination in air at 550 °C. Note that small features in the ^{27}Al NMR spectra at ~−17 and ~135 ppm, especially evident in the spectrum for the Si/Al = 6 sample, are spinning side bands.

assigned to framework, tetrahedral Al (Al_f) and the much weaker feature at ~0 ppm is attributed to extra-framework, octahedral Al. A simple peak area analysis gives Al_f/Al_{total} = 0.88. For the Si/Al = 12 sample, framework Al becomes more dominant with Al_f/Al_{total} = 0.98. For the Si/Al = 35 sample, essentially all Al stays as Al_f. Fig. 1(b) presents the corresponding ^{29}Si NMR results. For the Si/Al = 6 sample, features at −110, −104 and −99 ppm are attributed to Si(4Si, 0Al), Si(3Si, 1Al) and Si(2Si, 2Al), respectively [37,38]. For the Si/Al = 12 sample, no –Al–O–Si–O–Al– linkages exist and tetrahedral Si in Si(4Si, 0Al) and Si(3Si, 1Al) is observed at −111 and −105 ppm, where the former is more dominant as expected from the Si/Al ratio of 12. For the Si/Al = 35 sample, feature at −112 ppm assigned to Si(4Si, 0Al) becomes even more dominant, as compared to the Si(3Si, 1Al) feature at −105 ppm. the appearance of a SiO_2 phase is not unexpected. The XRD pattern for this sample shown in Fig. SI-1, however, indicates that the SiO_2 impurity does not possess a long range order.

3.2. H_2 temperature programmed reduction (H_2-TPR) results

Cu^{2+} ions located at different cationic sites have different binding energies with the framework; H_2-TPR provides a simple and direct measure of such differences. In our previous study, it was found that reduction of isolated Cu^{2+} to Cu^+ in Cu/CHA catalysts occurs below ~600 °C while Cu^+ reduction to Cu^0 occurs at much higher temperatures [15]. In the present study, H_2-TPR experiments were conducted only up to 650 °C to gain insight into the reduction behavior of Cu^{2+} as a function of Si/Al and Cu/Al ratios, and the results are plotted in Fig. 2. Experiments were conducted on both hydrated and dehydrated samples. Note that for the fully hydrated samples (samples stored at ambient conditions long enough to saturate with moisture), no other treatment was applied prior to TPR, except purging with helium at ambient temperature. For fully dehydrated samples, on the other hand, the samples were heated to 550 °C in dry 5% O_2/He, maintained at 550 °C for 30 min, and then cooled to ambient temperature in the same gas mixture prior to TPR.

Fig. 2(a) presents results for the series of Cu/SSZ-13 samples with Si/Al = 6. As shown in the lower panel for the hydrated samples, no reduction is found below ~300 °C for samples with very low Cu loadings (Cu/Al ⩽ 0.044), and a single, rather symmetric peak is found centered at ~380 °C. As Cu loading rises, a lower-temperature reduction peak develops at ~230 °C, and its intensity increases with increasing Cu loading. In the meantime, the high-temperature state shifts gradually to lower temperatures. This is especially the case for the two samples with the highest Cu loadings. Note also that, for samples displaying two reduction states, the low-temperature reduction state starts commonly at ~160 °C irrespective of Cu loadings. From the upper panel (for samples dehydrated in O_2 prior to TPR), no noticeable difference is found as compared to their hydrated counterparts for samples with the lowest Cu loadings (Cu/Al ⩽ 0.044). However for samples at intermediate Cu loadings (0.11 ⩽ Cu/Al ⩽ 0.29), the low-temperature state shifts to higher temperatures and partially converts to the high-temperature one. For the two highest Cu loading samples, one prominent finding is that the total H_2 consumption (as determined from the H_2 consumption peak areas) becomes substantially less for the dehydrated samples. This indicates that some Cu^{2+} species have already converted to Cu^+ during dehydration via a so-called "autoreduction" even in flowing O_2 atmospheres. This is important for our understanding of the relative stabilities of different Cu ion species as Si/Al ratios and Cu loading vary and more details will be given below. Note also that the onset of reduction for the dehydrated samples with the highest Cu loadings is as low as ~100 °C, considerably lower than that for the hydrated samples (~160 °C).

Fig. 2(b) and (c) presents TPR results for samples with Si/Al = 12 and 35, respectively. The hydrated Si/Al = 12 samples display two reduction states centered at ~240 and ~380 °C, resembling the Si/Al = 6 samples. However, the Si/Al = 35 samples only display one dominant reduction state at ~240 °C. TPR for dehydrated samples is more complicated. For the dehydrated Si/Al = 12 samples, as displayed in the upper panel of Fig. 2(b), the ~380 °C reduction state is similar to the corresponding hydrated samples, while for the Cu/Al = 0.13 and 0.23 samples, H_2 consumption at lower temperatures is apparently less than the corresponding hydrated samples. This again demonstrates that, during the dehydration process, a portion of Cu^{2+} converts to Cu^+ even in the oxygen flow.

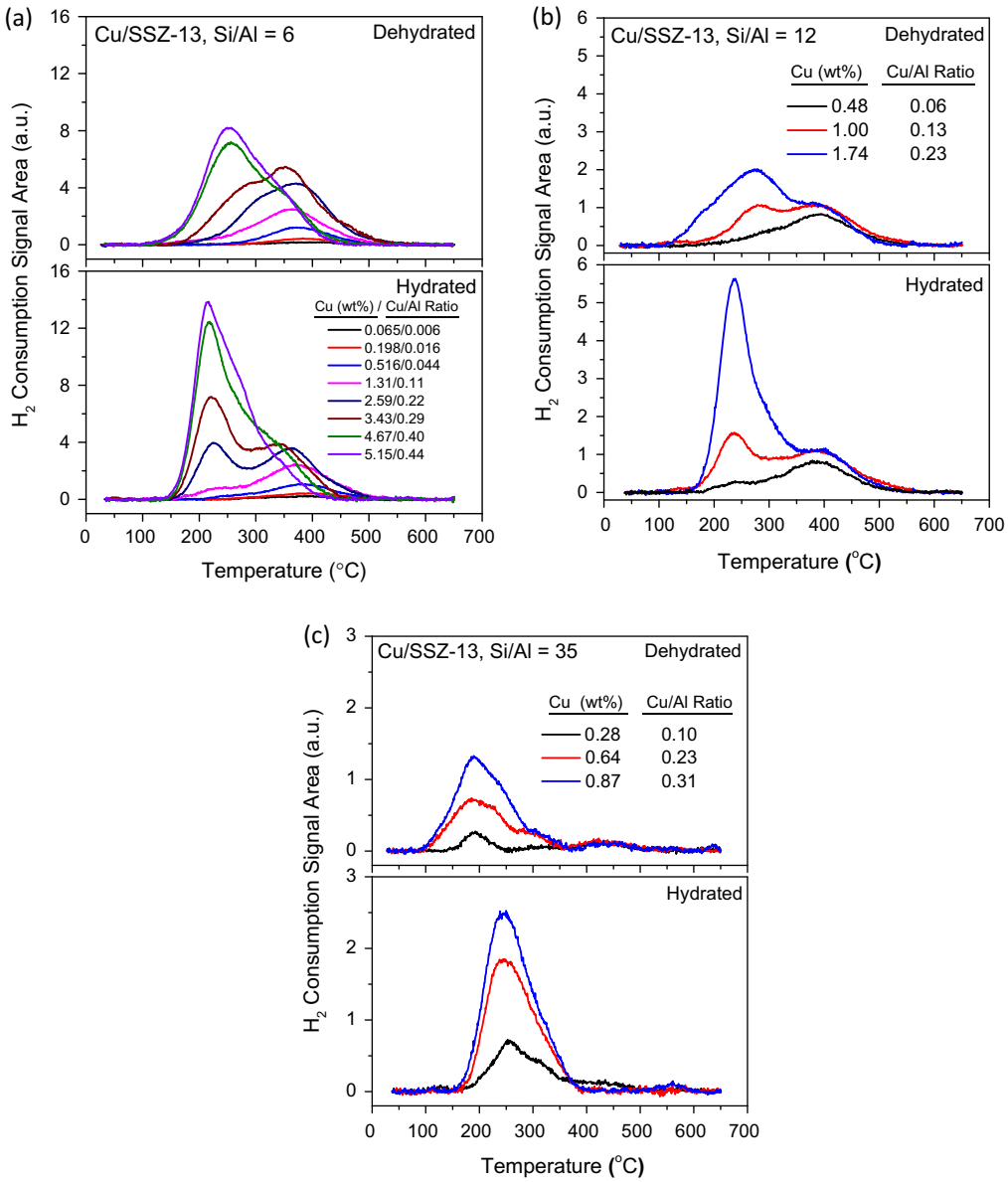

Fig. 2. Temperature-programmed reduction (TPR) data for Cu/SSZ-13 samples with various Cu loadings for (a) Si/Al = 6, (b) Si/Al = 12 and (c) Si/Al = 35. The upper panels show TPR for dehydrated samples while the lower panels show TPR for fully hydrated samples.

low-temperature reduction state is found at ~280 °C while a lower temperature state (seen as a shoulder) is also apparent at ~180 °C. For the dehydrated Si/Al = 35 samples (Fig. 2(c), upper panel), the sample with the lowest Cu loading (Cu/Al = 0.10) yields one weak reduction peak at ~180 °C. For the two samples with higher Cu loadings, the 180 °C reduction state also dominates. However, weaker but clear reduction states are also evident at ~240 and ~300 °C. Furthermore, it is important to note that for the latter samples, reduction starts as low as ~100 °C.

Fig. 3 presents H_2 consumption as a function of Cu loading for all *hydrated* samples (normalized to the same sample weight used in the TPR experiments). An excellent linear relationship is obtained in this case. Using CuO TPR as a calibration, H_2 consumption corresponds to $H_2/Cu = 0.5$ for all of the hydrated samples demonstrating that reduction below ~600 °C is due to the following reactions:

$$Cu^{2+} + 1/2\,H_2 \rightarrow Cu^{+} + H^{+} \quad (1)$$

Importantly, the good linear relationship rules out the existence of appreciable amounts of CuO clusters in any of our samples even at the highest Cu loadings. This follows since CuO is reduced directly to Cu^0 at ~300 °C, consuming two times the quantity of H_2 compared to reactions (1) and (2). This is consistent with our previous Electron Paramagnetic Resonance (EPR) spectroscopy analysis of these samples, where it was found that the majority of Cu species within our hydrated samples are EPR active (note that CuO clusters are EPR silent) [15]. For dehydrated samples, H_2 consumption is also determined in order to quantify the amounts of Cu^+ formed during dehydration via autoreduction. As shown in Table 3, for the Si/Al = 6 samples, no apparent autoreduction is found for samples with Cu/Al ⩽ 0.29. For the two higher Cu loading samples, more than 20% of Cu^{2+} is reduced to Cu^+ during dehydration. For the Si/Al = 12 samples, as with the Si/Al = 6 samples, the extent of autoreduction increases as Cu loading rises. Note that autoreduction becomes more facile for the Si/Al = 12 samples. For example, even the Cu/Al = 0.13 sample has 18% of Cu^{2+} autoreduced to Cu^+ during

DOCKET ALARM

Explore Litigation Insights

Docket Alarm provides insights to develop a more informed litigation strategy and the peace of mind of knowing you're on top of things.

Real-Time Litigation Alerts

Keep your litigation team up-to-date with **real-time alerts** and advanced team management tools built for the enterprise, all while greatly reducing PACER spend.

Our comprehensive service means we can handle Federal, State, and Administrative courts across the country.

Advanced Docket Research

With over 230 million records, Docket Alarm's cloud-native docket research platform finds what other services can't. Coverage includes Federal, State, plus PTAB, TTAB, ITC and NLRB decisions, all in one place.

Identify arguments that have been successful in the past with full text, pinpoint searching. Link to case law cited within any court document via Fastcase.

Analytics At Your Fingertips

Learn what happened the last time a particular judge, opposing counsel or company faced cases similar to yours.

Advanced out-of-the-box PTAB and TTAB analytics are always at your fingertips.

API

Docket Alarm offers a powerful API (application programming interface) to developers that want to integrate case filings into their apps.

LAW FIRMS
Build custom dashboards for your attorneys and clients with live data direct from the court.

Automate many repetitive legal tasks like conflict checks, document management, and marketing.

FINANCIAL INSTITUTIONS
Litigation and bankruptcy checks for companies and debtors.

E-DISCOVERY AND LEGAL VENDORS
Sync your system to PACER to automate legal marketing.